

Comparison between radial sensitivity of different strongly interacting probes

E. Friedman

The Racah Institute of Physics, The Hebrew University of Jerusalem, Jerusalem 91904, Israel

H. J. Gils and H. Rebel

*Kernforschungszentrum Karlsruhe GmbH, Institut für Angewandte Kernphysik,
D-7500 Karlsruhe, Federal Republic of Germany*

(Received 31 August 1981)

We investigate the radial sensitivity of different strongly interacting probes to neutron density distributions in nuclei. The experiments considered are elastic scattering of 104 MeV α particles, 1 GeV protons, 130 MeV pions, and also shifts and widths of pionic atom levels. The Fourier-Bessel method is used, thus avoiding any prior assumption on the neutron densities. To enable statistically meaningful comparisons between the different experiments, "pseudodata" are used, which are based on the real data. Although the region of most sensitivity is near the surface and is similar for each case, the α particles probe better the extreme surface and the protons probe better the interior. Pion scattering appears to be inferior to the other two scattering experiments because of the gradient terms in the potential. Surprisingly, there are some indications that π^+ could be better than π^- in determining neutron densities. Pionic atom data are sensitive mostly to the surface region. A critical discussion of error analyses is presented.

[NUCLEAR REACTIONS Radial sensitivity to neutron density
within optical model calculations of elastic $\sigma(\theta)$ data analyzed for α , p ,
 $\pi^\pm + {}^{48}\text{Ca}$ for 100–1000 MeV and of pionic atoms of ${}^{48}\text{Ca}$.]

I. INTRODUCTION

The radial distribution of nucleons in nuclei is a topic of current interest as it provides a sensitive test of theories of nuclear structure. While the distribution of protons can be studied most precisely via the electromagnetic interaction, studies of the total matter or neutron density distribution inevitably rely on a strongly interacting probe which implies more difficulties in interpreting experimental observations in terms of nuclear properties. Nevertheless, such probes have been shown to be quite useful in providing at least partial answers to the question of nuclear densities, in particular by comparative studies when the "apparatus function" (effective probe-nucleus interaction) could be "calibrated" on a nucleus with a presumably known neutron distribution. The results of various types of experiments such as elastic scattering of α particles, protons, or pions, etc. (see, for example, Ref. 1), although showing internal consistency, seem to be sometimes in conflict with each other. Apart from the residual uncertainty of the effective in-

teraction (which in most cases has not been taken into account in evaluating the errors of the final results) and in addition to deficiencies and constraints in the analysis itself, the above mentioned discrepancies could originate from differences in the radial sensitivity of different types of experiments which are currently used to probe the nuclear density distribution. It is therefore interesting to investigate which parts of the nucleus are well probed, and how uncertainties of the radial moments are affected by the radial sensitivity. Also important is a critical comparison of the methods of evaluating the uncertainties in the different analyses.

As previously demonstrated for α particle scattering,^{1,31,32} the radial sensitivity inevitably depends on the quality of the experimental data such as the range of momentum transfer or the angular and statistical accuracy. These can be quite different for different experiments even if one considers the best data available. In this paper we investigate the radial sensitivity which is presently accessible by different experiments. Therefore, the

studies are based on four experiments which are typical of their kind in the quality of the data they provide, thus characterizing the experimental state of art: (1) the elastic scattering of α particles² around 100 MeV, where only data extending to large angles are considered, thus probing the interior of the nucleus beyond the surface region; (2) the elastic scattering of protons in the GeV region,³ where the analysis in terms of the fundamental proton-nucleon interaction is a characteristic feature; (3) the elastic scattering of 130 MeV pions,⁴ where the availability of both π^+ and π^- beams together with the strong isospin dependence of the interaction are of particular interest; (4) strong interaction level shifts and widths in pionic atoms,⁵ where the very good experimental accuracy together with the isospin dependence of the interaction are interesting features for probing neutron distributions in nuclei.

Experiments on the elastic scattering of α particles and protons have been analyzed in recent years using methods which are efficient and instructive in studying the radial distributions of the interaction potential or the nuclear density. These methods, guided by the "model-independent" procedures used in electron scattering, overcome the constraints of using simple analytical forms and also provide a realistic analysis of the uncertainties in the studied distribution as a function of r , the distance from the center of nucleus. Several variants of these model-independent methods have been successfully used: (i) the Fourier-Bessel (FB) method,^{2,6,7} (ii) the sum-of-Gaussians (SOG) method,⁸ (iii) the spline function method,⁹ and (iv) a method based on a set of orthogonal polynomials.¹⁰ These methods could also be introduced into microscopic models^{7,11} relating the interaction potential to the density distribution of protons and neutrons in the nucleus. In the case of a zero-range probe-bound nucleon interaction, the potential is proportional to the nuclear density unless there are strong isospin effects which warrant separate handling of neutrons and protons (the latter distribution is generally assumed to be known from the accurately measured charge distribution). If a finite range is assumed for the interaction, the "microscopic" description implies some type of a folding model.^{11,12} Owing to the smearing effects of the folding integral, the densities are then more remote from the experimental data than are the potentials themselves, with the consequence that the relative uncertainties in the densities are larger than those for the potential,

particularly at the interior of the nucleus. All these features are clearly revealed when applying the "model-independent" procedures in the analyses of scattering data.

Unfortunately, it is not always possible to use these model-independent methods. For example, measurements of total or reaction cross sections yield one or two experimental numbers, and this is also the case when strong interaction level shifts and widths are measured in pionic atoms. Furthermore, model-independent analyses of the elastic scattering of pions at about 100 MeV do not seem to be fully justified at present owing to the insufficient knowledge of important details of the pion-nucleus potential.

In order to study the radial sensitivity of different types of experiments on equal footing we applied the FB method to all four experiments. Basically, the method consists of describing the neutron density distribution by a first approximation Fermi function plus a FB series, whose parameters are obtained from a best fit to the data. One of the merits of this method is that it provides realistic estimates of errors, thus enabling us to make meaningful comparisons of radial sensitivities. In Sec. II the method of the present analysis is described, particularly the generation of "pseudo-data" from the real data, which was chosen as a means of providing consistent comparisons between the different experiments. We mention that the FB method is applied here, for the first time, to analyze the elastic π^\pm scattering, and a procedure is given also for handling pionic atoms. Section III gives the results and Sec. IV contains a critical discussion of these results. It should be emphasized that all the present results, although referring to typical experimental data, are only for demonstration purposes, and they should not be regarded as final results of analyses for any of the experiments considered.

II. METHODS

The optical potentials for the various probes are related in one way or another (see below) to the nuclear densities. With the proton density distribution assumed to be known, we search for the neutron density distribution which is parametrized as follows

$$\rho_n(r) = \rho_{n_0}(r) + \sum_{k=1}^L \beta_k j_0(q_k r), \quad (1)$$

where $q_k = k\pi/R_c$ and the series is included in $\rho_n(r)$ only for $r < R_c$ where R_c is the cutoff radius. $\rho_{n_0}(r)$ is a first approximation to the neutron density and it has a volume integral of N , the neutron number. The coefficients β_k are obtained by requiring a best fit to the data while constraining the above series to have a zero volume integral. The following expression is obtained for the uncertainties⁶

$$\langle \Delta\beta_i \Delta\beta_j \rangle = 2(M^{-1})_{ij}, \quad (2)$$

where (M^{-1}) is the covariance matrix obtained numerically in the course of performing the χ^2 fit. This expression represents the statistical 67% confidence limit and is valid only in the case of purely statistical deviations between calculation and experiment, which implies a χ^2 per degree of freedom (χ^2/F) close to 1. When χ^2/F is larger than 1, it is a common practice to increase the quoted errors by multiplying Eq. (2) by χ^2/F which means that the error in, e.g., the various radial moments, are proportional to $(\chi^2/F)^{1/2}$. Whereas there is no rigorous justification to this prescription, particularly when the deviation of χ^2/F from 1 is due to some nonstatistical deficiency, it appears to be a plausible one at least when $\chi^2/F \lesssim 3$. In any case, when χ^2/F is considerably greater than 1, it is indicative of some fundamental problems in the analysis and a straightforward error analysis is inadequate. A detailed account of the error analysis is to be found in Ref. 13.

For the experimental results which are considered in the present work, and which are examples of "state of the art" results, the values of χ^2/F achieved in the best fits (in the present work and also by other methods) are not quite 1, but vary between 3 to $\cong 10$. Therefore, in order to avoid the above mentioned rescaling of errors, it was decided to use "pseudodata" with the only purpose of comparing the various types of experiments. The best-fit potentials were, therefore, used to calculate "experimental" results which were then shifted randomly according to the quoted real experimen-

tal errors. When fits were made to those pseudodata, values of χ^2/F of the order of unity were obtained. The nuclear densities used to generate these data are those calculated by Brown *et al.*¹⁴ The proton densities are in reasonably good agreement with results of electron scattering and the neutron densities are in fair agreement with results of elastic scattering of protons¹⁵ and α particles.¹⁶ These densities were consistently used throughout the present work.

For the case of pionic atoms a direct application of the FB method is not feasible, but we have approached that case by performing a combined analysis of pionic atoms and elastic scattering of α particles or protons. In the following we describe the potentials and types of calculations made for each of the four kinds of experiments. In each case we applied the type of analysis which is currently being used in interpreting experimental data, thus avoiding gross simplifications which could be introduced by adopting a common method for all experiments. Some simplifications were, however, made which are unlikely to affect the radial sensitivity, though they might be of importance in attempts of extracting nucleon densities from real data. Examples for such simplifications are the neglect of a spin-orbit interaction in proton scattering and choosing a particular type of potential for the pion experiments.

A. Elastic scattering of α particles

The fit to the data was made using the density-dependent folding model, which had been successfully applied to elastic α particle scattering extending to large angles.^{11,16} The real part of the potential was written as

$$\text{Re}U(r) = - \int V_{\text{eff}}(|\vec{r}' - \vec{r}|) \rho_m(r') d^3r' \quad (3a)$$

with the effective α particle-bound nucleon interaction being parametrized as a sum of a Gaussian (V_G, a_G) and a Yukawa (V_Y, a_Y) form

$$V_{\text{eff}}(|\vec{r}' - \vec{r}|) = [V_G \exp(-|\vec{r}' - \vec{r}|^2/a_G^2) + V_Y \exp(-|\vec{r}' - \vec{r}|/a_Y) / (|\vec{r}' - \vec{r}|/a_Y)] [1 - \gamma \rho_m^{2/3}(r')]. \quad (3b)$$

The term $[1 - \gamma \rho_m^{2/3}(r')]$ represents the density dependence of the α particle-bound nucleon interaction¹¹ where $\rho_m = \rho_n + \rho_p$ is just the sum of the neutron and proton densities. It has been found that a Gaussian plus Yukawa shape of the effective interaction fits the experimental cross sections better than the previously used pure Gaussian interaction^{11,16} due to the longer range of the Yukawa part. The parameters of the Gaussian part¹⁶ (as determined by the scattering on the "calibration" nucleus ^{40}Ca) showed only minor changes when including the Yukawa part. The characteristic quantities of the folded real optical potential

like depth, specific volume integral, rms radius, etc., are much closer to phenomenological approaches than without the Yukawa part. The imaginary potential was a conventional Woods-Saxon (WS) one, and it was also adjusted during the fits to the real data (see below) but not in the final FB fits to the pseudodata.

B. Elastic scattering of 1 GeV protons

It is commonly accepted that at energies of the order of 1 GeV one can reliably use the impulse approximation to obtain the proton-nucleus optical potential. The optical potential was therefore written as¹⁷

$$U(r) = \frac{\hbar^2 c^2}{(2\pi)^2 E_L} \int e^{-i\vec{q}\cdot\vec{r}} [f_n(q)F_n(q) + f_p(q)F_p(q)] d^3q, \quad (4)$$

where $f_{n(p)}$ are the proton-neutron (proton) scattering amplitudes and $F_{n(p)}$ are the nuclear form factors,

$$F_{n(p)}(q) = \int e^{i\vec{q}\cdot\vec{R}} \rho_{n(p)}(R) d^3R. \quad (5)$$

E_L is the total energy in the laboratory system, k_L and k_0 are the wave numbers in the laboratory and in the nucleon-nucleon systems, respectively. The dependence on the momentum transfer q was written as

$$f_{n(p)}(q) = f_{n(p)}(0) e^{-1/2\beta_{n(p)}^2 q^2} \quad (6)$$

and finally the optical theorem was used, namely,

$$f_{n(p)}(0) = \frac{k_0}{4\pi} \sigma_{T_{n(p)}} (i + \alpha_{n(p)}). \quad (7)$$

An additional kinematical factor and the $(A-1)/A$ factor¹⁷ were included in $U(r)$ but not written in Eq. (4) for simplicity. In any case, these factors are not essential in the present application because the amplitudes were slightly adjusted in order to improve the fit to the data. In the calculations the Fourier transformation in Eq. (4) was not performed explicitly. Instead, a Gaussian folding was performed in coordinate space,¹⁸ where Eq. (4) becomes

$$U(r) = \frac{\hbar^2 c^2 k_L}{2E_L} (2\pi)^{-3/2} \int \{ \rho_n(r') (i + \alpha_n) \sigma_{T_n} \exp[-|\vec{r}' - \vec{r}|^2 / 2\beta_n^2] \\ + \rho_p(r') (i + \alpha_p) \sigma_{T_p} \exp[-|\vec{r}' - \vec{r}|^2 / 2\beta_p^2] \} d^3r'. \quad (8)$$

Not included in the present calculation was a spin-orbit term, but that should not affect our results regarding radial sensitivity because of the small adjustments to the parameters mentioned above made before producing the pseudodata, so that a best fit to real data was first achieved.

C. Elastic scattering of pions

In recent years the zero-energy π^- -nucleus potential has been thoroughly studied with the help of very precise results for strong interaction level shifts and widths in pionic atoms.^{5,19,20} Some applications have already been made²¹ of such refined potentials in the analysis of elastic scattering of pions at low energies. This potential, which is inserted into the Klein-Gordon equation, is given by

$$U(r) = \frac{1}{2\mu} [q(r) + \vec{\nabla}\cdot\alpha(r)\vec{\nabla}], \quad (9)$$

where μ is the reduced mass, q is the s -wave (local) part, and α the p -wave (momentum dependent) part of the potential, written in terms of the nuclear densities as follows:

$$q(r) = -4\pi \left\{ \left[1 + \frac{\mu}{m} \right] [b_0(\rho_n + \rho_p) + b_1(\rho_n - \rho_p)] + \left[1 + \frac{\mu}{2m} \right] 4B_0\rho_n\rho_p \right\}, \quad (10)$$

$$\alpha(r) = \frac{\alpha_0(r)}{1 + \frac{1}{3}\alpha_0(r)}, \quad (11)$$

$$\alpha_0(r) = 4\pi \left\{ \left[1 + \frac{\mu}{m} \right]^{-1} [c_0(\rho_n + \rho_p) + c_1(\rho_n - \rho_p)] + \left[1 + \frac{\mu}{2m} \right]^{-1} 4C_0\rho_n\rho_p \right\}. \quad (12)$$

m is the nucleon mass and the coefficients b_0 , b_1 , B_0 , c_0 , c_1 , and C_0 are usually taken from fits to data.²⁰

Additional terms due to the so-called angle transformation and due to $\vec{l} \cdot \vec{\sigma}$ interaction²⁰ have not been written in the above potential, and although they have been included in some analyses,²¹ they have been excluded from the present work since they are unlikely to be relevant to the radial sensitivity.

The above potential assumes a zero range for the pion-nucleon interaction. Introducing a finite range to the p -wave part of Eq. (9) may have, in principle, far reaching consequences.²² However, it was shown recently by Alexander *et al.*²³ that for pionic atoms the only effect of introducing finite range is to change the values of the parameters, while maintaining the same overall picture. We therefore used in this work the zero-range version of the potential, but it is possible that folding in a finite (short) range could reduce the sensitivity observed.

D. Pionic atoms

The strong interaction level shifts and widths in pionic atoms are, in principle, another source of information on nuclear densities. In this case the experimental information consists of just two numbers and one cannot use a method such as the FB one. Previous attempts to extract information on neutron densities from pionic atoms relied on an analytic form for the densities. This is exactly what we avoid in the present work.

The method adopted here is simply to include the pionic atoms results in a combined analysis of α particle or proton scattering. To the χ^2 of the scattering problem we add the contribution due to the pionic atom, namely,

$$\chi_\pi^2 = [(\epsilon_{\text{exp}} - \epsilon_{\text{calc.}})/\Delta\epsilon]^2 + [(\Gamma_{\text{exp}} - \Gamma_{\text{calc.}})/\Delta\Gamma]^2, \quad (13)$$

where ϵ and Γ are the strong interaction level shift and width, respectively, $\Delta\epsilon$ and $\Delta\Gamma$ being the ex-

perimental errors. The nuclear densities which enter the pionic atom calculations are those appearing in the scattering problem. This method of a combined analysis of two different experiments had already been successfully used²⁴ with real data. In the present work it was found to perform remarkably well.

III. RESULTS

In order to enable a comparison between the four types of experiments, the same nucleus — ⁴⁸Ca — was chosen for all cases. This nucleus has been extensively studied by many different groups using a variety of methods and good quality data are available for the present studies. This nucleus with its relatively large neutron excess is typical of medium-weight to heavy nuclei, which form the prime object of investigations of neutron density distributions.

A. Elastic scattering of α particles

The data on which the present sensitivity tests are based are those from Karlsruhe² which were extensively analyzed using the FB method.^{2,11,13} Although the final FB analyses were applied to pseudodata we proceeded as far as possible in the same way as in analyses of real data aiming at information about neutron densities.

First, the elastic scattering cross sections for $\alpha + ^{40}\text{Ca}$ were used to adjust the parameters V_G , a_G , and γ of the effective α particle-bound nucleon interaction. (V_Y and a_y were kept fixed according to the results of previous analyses.) Turning then to ⁴⁸Ca the real part of the optical potential was fixed according to the standard densities and the interaction determined as described above. The parameters of the imaginary part were varied in order to fit the experimental data. The quality of the fit is characterized by $\chi^2/F = 8$, which is of the same order as that obtained for the other scattering experiments by similar procedures (see below). The theoretical angular distribution resulting from this fit was then used as a basis for dis-

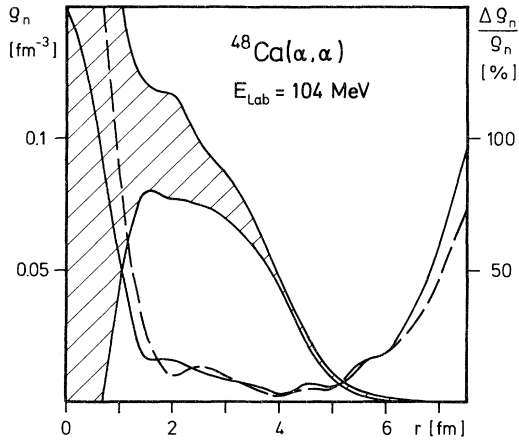


FIG. 1. Neutron density distribution of ^{48}Ca and its percentage errors as determined from the elastic scattering of 104 MeV α particles. The shaded area represents the range of uncertainty in the density. The solid and dashed curves represent the percentage error when a separate or combined analysis is made of α scattering and pionic atoms, respectively. (See Sec. III D.)

tributing pseudodata randomly about it at all angles measured and assuming the real experimental errors. The pseudodata were again reproduced with a χ^2 -value per point of 0.7.

For the subsequent FB fits to the pseudodata a first approximation of the neutron density ρ_{n_0} [Eq. (1)] of the Fermi form was assumed. Its two parameters c and a were adjusted using the pseudodata yielding $\chi^2/F=0.8$.

Finally, only the FB coefficients were varied in order to fit the pseudodata. The number of varied FB terms ranged from 4 to 6 and the cutoff radius R_c from 6.5 to 9 fm. χ^2/F values of 0.7 were obtained. Although, even with $R_c=9$ fm, the errors of the density itself and its various integral moments did not increase unreasonably (as observed for other projectiles), the final results only contain calculations including cutoff radii up to $R_c=7.5$ fm.

In Fig. 1 the error band (shaded area) containing the resulting neutron density and its percentage er-

ror (solid curve) are displayed. (The dashed curve is discussed in Sec. III D.) It is obvious that the α particles are not able to probe the neutron density at radii smaller than 1.5 fm, whereas good sensitivity is observed even at distances where the density is less than 1% of the central value. It should be noted that the input neutron density¹⁴ used for the preparation of pseudodata fully lies inside the error band and also its structure around $r \sim 2$ fm is reproduced although a smooth Fermi distribution was used for ρ_{n_0} in Eq. (1).

As examples of integral quantities related to the neutron density, various radial moments have been computed. The root mean square (rms) radius and its error are given in Table I together with those obtained from analyses of the other experiments. For the present α particle scattering analyses (using pseudodata) the absolute error of the rms radius is one of the largest as compared to the errors of higher radial moments. Even the 6th moment is better determined than the rms radius.

Out of the experiments treated in this paper the scattering of α particles is the only one where the FB method has been extensively applied also to real data. Comparing both types of results with regard to the resulting radial sensitivities [characterized, e.g., by the percentage error of the density (see Fig. 1)] one can state that they are qualitatively the same. Even quantitatively, there are only minor differences, in particular in the region $r=3-5$ fm. At small radii the errors determined from the real data in many cases are even smaller than those determined from the pseudodata. However, the spread of the results of many calculations with real data using different numbers of FB terms and different cutoff radii (which is negligible for pseudodata) also show the poor accuracy of the determination of the densities in the interior. The errors of the radial moments extracted from the analyses of real data are a factor of 2-3 larger than for the pseudodata.

The fact that some errors determined from real data can be smaller than obtained from pseudodata

TABLE I. Root-mean-square radii obtained from the different analyses. All values are in units of fm.

Input value	100 MeV α scattering	1 GeV proton scattering	130 MeV π^+ scattering	130 MeV π^- scattering	50 MeV π^+ scattering	50 MeV π^- scattering	Pionic atoms and α scattering	Pionic atoms and proton scattering
3.581	3.58 ± 0.03	3.54 ± 0.04	3.58 ± 0.03	3.55 ± 0.17	3.55 ± 0.16	3.49 ± 0.20	3.58 ± 0.03	3.55 ± 0.03

indicates the remaining deficiencies of the reaction model which is not able to reduce the analysis of the scattering problem to a purely statistical treatment.

B. Elastic scattering of 1 GeV protons

The experimental cross sections used for the analyses of high energy proton scattering are due to the Saclay-Gatchina group.³ The potential of Eq. (4) was used in analyzing the results for ^{40}Ca adjusting the total neutron cross section σ_{T_n} and the ratio of the neutron imaginary to real part. Only minor adjustments (of the order of 10–20%) were required in order to get a χ^2/F of 6.4. Keeping all parameters then fixed, the angular distribution for the scattering of 1.04 GeV protons by ^{48}Ca was calculated reproducing the experimental data with $\chi^2/F=12$. Subsequently, the pseudodata were generated in the same way as for the α particle scattering. The details of the FB fits were also the same as for the α particle scattering case. The resulting neutron density and its error band is displayed in Fig. 2. (For the discussion of the dashed line see Sec. III D.) In contrast to the α particle scattering, the protons show a remarkable sensitivity even to the very interior region of the target nucleus and also the slope is slightly better determined than by the α particle scattering. However, due to the shorter range of the interac-

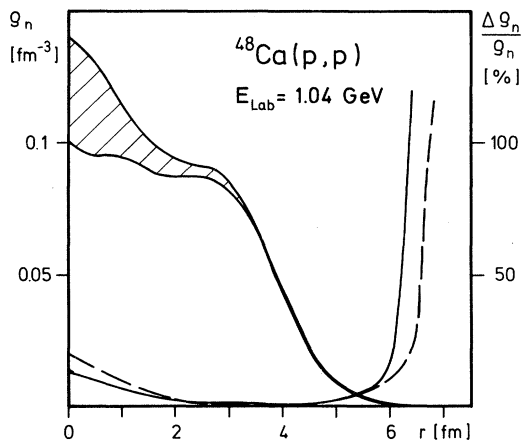


FIG. 2. Neutron density distribution of ^{48}Ca and its percentage errors as determined from the elastic scattering of 1 GeV protons. The shaded area represents the range of uncertainty in the density. The solid and dashed curves represent the percentage error when a separate or combined analysis is made of proton scattering and pionic atoms, respectively (see Sec. III D).

tion compared to the effective α particle interaction, and due to the weaker absorption, the accuracy of the derived density rapidly deteriorates at $r \cong 6.5$ fm. As a consequence the radial moments M^K are less accurately determined for $K > 1$ as compared to the α particle scattering (Table I). For M^6 the error is more than a factor of 2 larger as compared to the α particle scattering case. The input neutron density¹⁴ again fully lies inside the error band and its structure is reproduced.

C. Pion scattering

The experimental results which form the basis of the present work are those of Gretillat *et al.*⁴ at 130 MeV. No detailed analysis has yet been made of these data in terms of the full pion-nucleus potential [Eqs. (9)–(12)]. However, in order to generate the pseudodata needed for the present work, we have analyzed the real data using a simplified form of the potential, where the Lorentz-Lorenz effect was not taken into account [Eq. (11)] and also with $\text{Re}B_0$ and $\text{Re}C_0$ set to zero. An initial fit to ^{40}Ca was not made in this case because such a fit is unable to determine the coefficients b_1 and c_1 [Eqs. (10–12)]. Although this analysis is only preliminary, it was noticed that the π^- data determine essentially the momentum dependent part of the potential (α) and the π^+ data determine the local part (q). Values of χ^2/F of 7 for π^- and 18 for π^+ were obtained for the real data, which are not much worse than what is achieved in the initial phases of analysis of other scattering experiments. The potential parameters so obtained did not show the expected isospin relationship. However, with

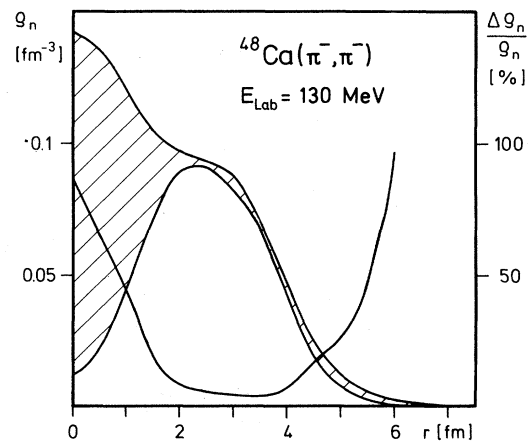


FIG. 3. Neutron density distribution (shaded area) and its percentage errors (solid curve) for ^{48}Ca obtained from the elastic scattering of 130 MeV π^- scattering.

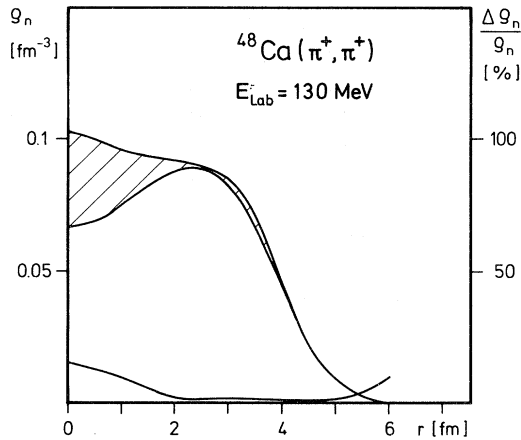


FIG. 4. Results for 130 MeV π^+ scattered by ^{48}Ca . See also caption to Fig. 3.

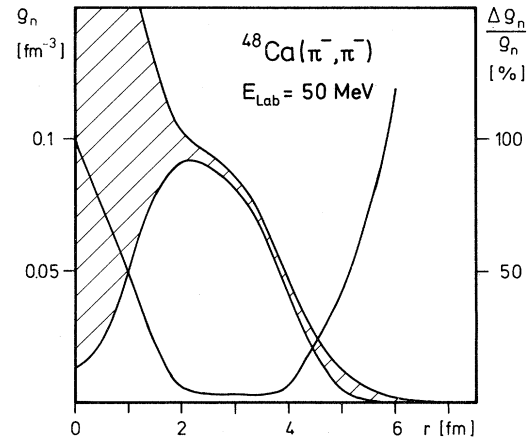


FIG. 5. Results for 50 MeV π^- scattered by ^{48}Ca . See also caption to Fig. 3.

this reservation in mind, these potentials were used to generate the pseudodata, where, obviously χ^2/F was of the order 1. Figures 3 and 4 show the neutron densities obtained from FB analyses. The sharp contrast between the accuracies obtained in the two cases can be traced to the relative importance of the local and momentum dependent terms in the potential. In the π^+ potential, the local part is dominant, hence the overall picture is rather similar to that found for the scattering of protons. On the other hand, in the π^- potential the nonlocal part, with its derivative terms, plays a major role and that has a most negative effect on the ability to derive densities from the data, when a method such as the FB one is being used. We emphasize again that the fit to the real data may not be unique, hence the conclusions regarding the relative sensitivity of the π^+ and π^- may not be final. However, the conclusions regarding the damaging effect of the nonlocal component of the potential on the determination of densities are probably rather general.

As a further check on this point we turned to 50 MeV, where it has been shown²¹ that potentials derived from fits to pionic atoms are quite adequate. Unfortunately, we are unaware of experimental results for ^{48}Ca , so we generated pseudodata using the pionic atoms potential I given by Friedman and Gal.^{20,25} In this potential it is found that the relative strength of the momentum dependent term is greater for π^- than for π^+ . Figures 5 and 6 show the results for 50 MeV π^\pm scattering and indeed it is seen that the π^+ are slightly better able to determine nuclear densities than are the π^- .

D. Pionic atoms

The experimental results on which the present sensitivity tests of pionic atoms are based are those of Powers *et al.*⁵ for the $2p$ level in pionic ^{48}Ca . Using potential III of Friedman and Gal,²⁰ with slightly revised parameters,²⁵ the calculated strong interaction level shifts and widths agree with the experimental results when using the densities of Ref. 14. Hence, there was no need to generate pseudodata for the pionic atoms case.

As described in Sec. IID combined analyses of pionic atoms and either elastic scattering of α particles or protons have been made using the same proton and neutron distributions for all experiments and varying the FB coefficients of the neu-

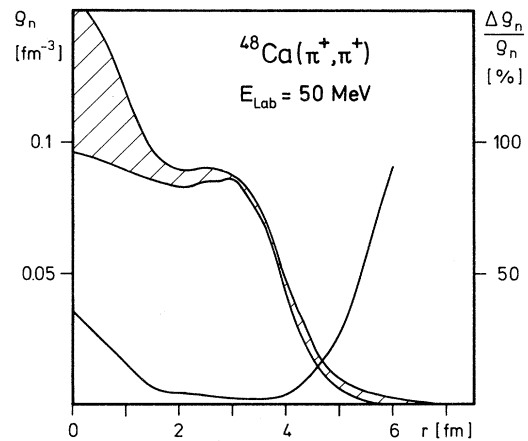


FIG. 6. Results for 50 MeV π^+ scattered by ^{48}Ca . See also caption to Fig. 3.

tron distribution. In contrast to corresponding analyses of real data of α particle scattering²⁴ the constraint provided by the pionic atoms results was less pronounced here due to the relatively larger weight carried by the scattering pseudodata. However, the effect of the pionic atoms data on the resulting densities and particularly on their errors is clearly demonstrated by the dashed curves in Figs. 1 and 2 and by the rms radii and their errors quoted in Table I. It is obvious that the sensitivity curve given by the relative error of the neutron distribution is shifted to larger radii in both cases. This indicates a dominant sensitivity of the pionic atoms data to the radial region at about $r \cong 5-6$ fm. As a consequence of this sensitivity to large radii only the error of the rms radius from the proton scattering could considerably be reduced by the combined analysis. In fact, for higher moments than M^2 , even a stronger reduction of the errors is observed.

In the case of the pionic atoms analysis combined with α particle scattering the trend of shifting the sensitivity curve to larger radii is observed (Fig. 1). However, the determination of the various radial moments is not improved. On the contrary, moments M^K with $K > 4$ are less accurately determined as compared to the α particle analyses without pionic atoms. This could be a hint that the π^- bound in pionic atoms probe the neutron distribution only in a very limited region around $r = 5$ fm.

IV. DISCUSSION

The purpose of the present study was to explore which regions of the neutron density distribution are determined from experiments using different strongly interacting probes. We considered four kinds of typical examples of current interest. In order to get a realistic picture it was important to analyze each kind of experiment within its own specific theoretical description, as oversimplifications might lead to conclusions which reflect rather the limits of the approximation and not those of the experiments.

The two major questions which are being asked when comparing the sensitivities to the neutron distribution are: (i) What is the radial region in which the density is well determined by the experiment and (ii) to what accuracy can the density be determined either locally or preferably in terms of integral quantities such as radial moments? The

answer to the first question can be found by inspecting Figs. 1–6 where it is seen that all experiments are sensitive to the neutron density in roughly the same region of 2–5 fm, or from the middle of the internal plateau to the point where the density is $\sim 10\%$ of its central value. The scattering of 130 MeV π^- is definitely inferior compared to the other methods, as a source of information on neutron densities, because of the importance of the momentum dependent term in the potential. It is also clear that the outer regions of the densities are better determined by α particles than by protons and the opposite is true for the interior. Although we have used pseudodata in this work, these conclusions concerning the radial range of sensitivity are most likely reflecting the real situation as given in current analyses of elastic scattering of α particles¹⁶ and of protons.^{15,26}

The answer to the second question is considerably more complex. Table I summarizes values of the rms radius of the neutron distribution obtained from the different experiments and these results are also typical of other radial moments. It is reassuring to see that in all cases the resulting value of rms radius agrees, within the calculated uncertainty, with the input value used to generate the pseudodata. Despite the large differences in the errors of the densities in the interior obtained from proton scattering and α particle scattering (Figs. 1 and 2), both experiments determine the rms radius to the same accuracy because it is dominated by the densities close to the surface. The considerably larger errors found for 50 MeV π^\pm and for 130 MeV π^- result from the important role played by the momentum dependent component of the potential [Eq. (9)] with its derivative terms. As mentioned above, the conclusions regarding 130 MeV π^+ could be fortuitous, but they nevertheless serve as a useful demonstration of the improvement expected when the role of the momentum dependent component is reduced. Since the π^\pm optical potentials used here are better justified at lower energies, the results for 50 MeV pion scattering are probably quite reliable. The fact that the π^+ seem to probe the neutrons in the central region more sensitively than the π^- is somewhat surprising at a first glance. However, as just the π^+ interact more weakly with the surface neutrons than the π^- do, they have a good chance to penetrate deeper into the nucleus.

When we turn to real data, the details of Table I are likely to change. As typical values of χ^2/F achieved are between 3–10, the errors in the den-

sity are expected to increase by a factor of 2 to 3. In addition, errors of the model itself will have to be included and in that respect there exist differences between the various probes. In the case of protons the spin-orbit term will complicate matters, whereas in the case of pions the great complexity of the potential will undoubtedly increase the uncertainties even further. For α particles, which have vanishing spin and isospin, the imaginary potential is treated phenomenologically (unlike in the other cases), thus introducing additional uncertainties. Based on extensive analyses of the scattering of α particles^{2,11,13,16} we estimate that in all experiments the rms radius is never determined to better than ± 0.15 fm, when including the uncertainties due to the effective interaction. In the case of pionic atoms, the full power of the combined analysis of strong interaction level shifts and widths together with a scattering experiment, is more clearly observed²⁴ with real data, where the pionic atom data have larger relative weight and the constraints due to the pionic atoms reduce the errors obtained from the scattering experiment.

Returning to the question of why different experiments yield different results, it seems unlikely that the small differences in radial sensitivity are the origin of the discrepancies in the quoted values of rms radii. A more likely explanation can be found in the inadequate analysis of uncertainties (including those of the effective interaction) combined with the constraints in some analyses, in particular those introduced by the use of simple parametrizations²⁷ of ρ_n . For example, the 1 GeV proton scattering result²⁸ of the Saclay group based on a three-parameter Fermi shape of ρ_n which yields $\langle r^2 \rangle_n^{1/2} - \langle r^2 \rangle_p^{1/2} = 0.10 \pm 0.03$ fm for ^{48}Ca seems to contradict the α particle scattering result¹⁶ of $\langle r^2 \rangle_n^{1/2} - \langle r^2 \rangle_p^{1/2} = 0.25 \pm 0.12$ fm derived by a FB description of ρ_n . However, when comparing the densities in the well-determined region of ρ_n obtained in the two experiments, one finds that there is no significant difference. This is a strong hint that the quoted error in the proton scattering result does not reflect the uncertainties in the less well-determined part of ρ_n . In fact, the use of model-independent techniques in proton scattering analyses¹² has led recently to more consistent results and more realistic errors.

Further comments on the pitfalls of using simple analytical forms for ρ_n are in order. It is obvious that when the data determine the density only over a limited region of space, the density in other parts will be given by an analytic continuation of the

prechosen function, which will then lead to gross underestimates of errors. Another method of studying radial sensitivities, e.g., that of introducing a "notch" into the density,^{29,30} is equally unreliable. Although this method more or less correctly locates^{30,31} the radial regions of sensitivity in the case of smooth potentials, it is totally unable to supply information on the accuracies of the results and their dependence on the quality of data (see, e.g., Ref. 32). The failure of the notch test is spectacular in the case of pion scattering³¹ where it leads to opposite results than obtained by the FB method. This is due to the fact that the notch essentially perturbs the momentum dependent part of the potential, thus simulating sensitivity mainly for π^- and less for π^+ .

Certainly, the FB method is not the only one which is suitable for model independent studies of nuclear densities and of the uncertainties involved. Another method which was recently used to estimate the uncertainties^{12,33} is based on introducing long-range perturbations into the density and finding the limits of these such that any calculated point will not deviate beyond its estimated experimental error. In principle, this method corresponds to the FB statistical approach, based on an increase of χ^2 by 1. However, when χ^2/F is significantly larger than 1, this method leads to much smaller estimated errors as compared to the covariance matrix method.

As a general rule, the best value of χ^2/F achieved in analyzing experimental data should be used as a guide to possible systematic errors. Obviously when χ^2/F approaches 1 the different methods of evaluating uncertainties should be equivalent. With these comments in mind we note that while values of χ^2/F achieved³³ in some of the analyses are of the order of 10, the errors quoted are as though χ^2/F was 1, which may lead to unrealistically small errors.

In conclusion, we have demonstrated rather similar radial sensitivity to neutron distributions for 100 MeV α particles and 1 GeV protons, with better sensitivity for the former at large radii and for the latter at small radii. The radial sensitivity of pions is smaller and is hampered by the momentum dependent component of the potential with its derivative terms. The apparent disagreement between results from different experiments is probably due to underestimating of the errors involved.

We would like to thank (Professor) Dr. G. Schatz for his interest and Dr. C. J. Batty for stimulating discussions.

- ¹Proceedings of the International Discussion Meeting, Karlsruhe, 1979, edited by H. Rebel, H. J. Gils, and G. Schatz, Kernforschungszentrum Karlsruhe Report KfK 2830, 1979.
- ²H. J. Gils, E. Friedman, H. Rebel, J. Buschmann, S. Zagromski, H. Klewe-Nebenius, B. Neumann, R. Pesl, and G. Bechtold, Phys. Rev. C 21, 1239 (1980).
- ³G. Bruge, Saclay, Department de Fisica Nucleaire Report DPh-N/ME/78-1, 1978 (unpublished).
- ⁴P. Gretillat, J. P. Egger, R. Corfu, J. -F. Germond, C. Lunke, E. Schwarz, C. Perrin, and B. M. Freedom, Nucl. Phys. A364, 270 (1981).
- ⁵R. J. Powers, K. -C. Wang, M. V. Hoehn, E. B. Shera, H. D. Wohlfahrt, and A. R. Kunselman, Nucl. Phys. A336, 375 (1980).
- ⁶E. Friedman and C. J. Batty, Phys. Rev. C 17, 34 (1978).
- ⁷I. Brissaud and X. Campi, Phys. Lett. 86B, 141 (1979).
- ⁸I. Brissaud and M. K. Brussel, J. Phys. G 3, 481 (1977).
- ⁹L. W. Put and A. M. J. Paans, Nucl. Phys. A291, 93 (1977).
- ¹⁰P. L. Roberson, Phys. Rev. C 22, 482 (1980).
- ¹¹E. Friedman, H. J. Gils, H. Rebel, and Z. Majka, Phys. Rev. Lett. 41, 1220 (1978).
- ¹²L. Ray, Phys. Rev. C 19, 1855 (1979).
- ¹³H. J. Gils, E. Friedman, H. Rebel, J. Buschmann, S. Zagromski, H. Klewe-Nebenius, B. Neumann, R. Pesl, and G. Bechtold, Kernforschungszentrum Karlsruhe Report KfK 2838, 1979.
- ¹⁴B. E. Brown, S. E. Massen, and P. E. Hodgson, J. Phys. G 5, 1455 (1979).
- ¹⁵L. Ray and P. E. Hodgson, Phys. Rev. C 20, 2403 (1979).
- ¹⁶H. J. Gils, E. Friedman, Z. Majka, and H. Rebel, Phys. Rev. C 21, 1245 (1980).
- ¹⁷A. K. Kerman, H. McManus, and R. M. Thaler, Ann. Phys. (N.Y.) 8, 551 (1959).
- ¹⁸C. J. Batty and E. Friedman, Nucl. Phys. A179, 701 (1972).
- ¹⁹C. J. Batty, S. F. Biagi, E. Friedman, S. D. Hoath, J. D. Davies, G. J. Pyle, G. T. A. Squier, D. M. Asbury, and A. Guberman, Nucl. Phys. A322, 445 (1979).
- ²⁰E. Friedman and A. Gal, Nucl. Phys. A345, 457 (1980).
- ²¹K. Stricker, H. McManus, and J. Carr, Phys. Rev. C 19, 929 (1979).
- ²²V. B. Mandelzweig, A. Gal, and E. Friedman, Ann. Phys. (N.Y.) 124, 124 (1980).
- ²³Y. Alexander, A. Gal, V. B. Mandelzweig, and E. Friedman, Nucl. Phys. A356, 307 (1981).
- ²⁴E. Friedman and H. J. Gils, Ninth International Conference on High Energy Physics and Nuclear Structure, Versailles, 1981 (unpublished), p. 137.
- ²⁵E. Friedman, Phys. Lett. 104B, 357 (1981).
- ²⁶L. Ray, Nucl. Phys. A335, 443 (1980).
- ²⁷H. O. Meyer, Phys. Rev. C 17, 1116 (1978).
- ²⁸S. Shlomo and R. Schaeffer, Phys. Lett. 83B, 5 (1979).
- ²⁹N. S. Wall, A. A. Cowley, R. C. Johnson, and A. M. Kobos, Phys. Rev. C 17, 1315 (1978).
- ³⁰J. G. Cramer and R. M. De Vries, Phys. Rev. C 22, 91 (1980).
- ³¹H. J. Gils, E. Friedman, and H. Rebel, Kernforschungszentrum Karlsruhe Report KfK 3039, 1980.
- ³²E. Friedman, H. J. Gils, H. Rebel, and R. Pesl, Nucl. Phys. A363, 137 (1981).
- ³³L. Ray, private communication.